JOURNAL OF COMPUTATIONAL PHYSICS 17, 19–52 (1975)

Numerical Calculation of Multiphase Fluid Flow*

FRANCIS H. HARLOW AND ANTHONY A. AMSDEN

University of California, Los Alamos Scientific Laboratory, Los Alamos, New Mexico 87544

Received July 9, 1974

A new computing technique is described for the solution of fluid flow problems in which several fields interpenetrate and interact with each other. An implicit coupling for each field between mass transport and equation of state allows for calculations in all flow-speed regimes, from far subsonic (incompressible) to far supersonic. In addition, the momentum transport between fields is implicit, allowing for all degrees of coupling, from very loose to completely tied together. Phase transitions permit interchange of mass, momentum and energy between fields, each of which is composed of several components. Considerable generality is present, to permit application to a wide scope of complicated problems, for example, the fluidized dust bed, the flow of a liquid with entrained bubbles, and atmospheric condensation with the fall of precipitation.

INTRODUCTION

The presence of bubbles, droplets or chunks in a fluid introduces the potentiality for relative motion, and accordingly requires more than one set of field variables for specification of the dynamics. Examples of such circumstances are given by:

(1). cavitating or flashing flow, in which bubbles are formed of vapor of the fluid itself,

(2). the fluidized dust bed, in which liquid or vapor rises through a bed of solid grains;

(3). precipitation with snow, hail or rain falling through the atmosphere;

(4). jet entrainment, in which immiscible or mutually diffusing liquid droplets are carried and mixed with another liquid.

In each case, there is relative motion between the two fields, together with the interchange of momentum and possibly heat. In many cases there also is an exchange of mass through phase transitions or the effects of burn or other chemical reactions, as for example, in the burning of granules of gunpowder.

* This work was performed under the auspices of the US Atomic Energy Commission.

The coupled differential equations for such processes have been formulated by various authors for a variety of circumstances, but the techniques for their efficient and accurate solution have scarcely developed beyond applicability to the most simplified problems. Our purpose is to show how the differential equations can be implicitly coupled in a finite-difference representation that is highly versatile for the solution of time-varying problems in several space dimensions. We refer to this new technique as an implicit, multifield (IMF) solution method. Among its properties are the following:

(1). implicit treatments of mass convection and equation of state, so that flow speeds can range from far subsonic (incompressible) to supersonic;

(2). implicit coupling among the fields, to allow forces that range from very weak to those strong enough to completely tie the fields together;

(3). energy equations that allow for heat production from condensation, nuclear reactions, exothermic chemistry, etc.;

(4). interchange of materials from one field to another, for example, through phase transitions;

(5). the allowance for inhomogeneity in the composition and other material properties of the field;

(6). the capability for pile up of a particulate field into a close-packed region with variable boundary position;

(7). a representation of material strength, so that a porous field may resist deformation until softened by heating or yielding under excessive strain;

(8). a transport equation for particulate, droplet or bubble scale, representing such processes as fragmentation, coalescence and expansion or contraction.

The basic numerical procedure is an extension of the implicit, continuous-fluid, Eulerian (ICE) technique [1], which allows for fluid dynamics studies at all flow speeds. Although the technique has been applied to generalized Eulerian–Lagrangian representations [2], the present multiphase flow version is restricted to a purely Eulerian mesh of computational cells. A Lagrangian mesh in the usual sense cannot be uniquely defined because of the separate and distinct fields of material velocity. We illustrate the technique with a two-field version in cylindrical coordinates with azimuthal symmetry. For brevity, the interactions between fields are here described by relatively simple expressions. Such simplifications are easily removed, however, as discussed in the text and illustrated by some of the test problems that have been solved with the technique.

The Differential Equations

Numerous publications have described the equations necessary for multifield flow, usually under the headings "two-phase flow" and "fluidization." A surprising amount of disagreement exists on the proper representation by continuum equations of the dynamics of such a system, especially concerning the proper coupling between the two fields. The form we use is based on elements derived from Murray [3], Soo [4], Nigmatulin [5], Anderson and Jackson [6], Kalinin [7], and Mecredy and Hamilton [8]. We designate the two fields as "vapor" and "droplets," the former a gas in bubble form or with dispersed droplets in it, the latter a fluid or aggregate of solid particles. Subscripts referring to the vapor and droplet fields are, respectively, v and d; within each field we allow for two components, designated by subscripts 1 and 2. The nomenclature employed for the field variables is, in part, the following:

$\mathbf{u}$ = velocity, with components u and v in the cylindrical-coordinate directions r and z, respectively,

ρ = material density, the actual microscopic mass per unit volume of a particular material,

ρ' = macroscopic material density, the mass of material per unit total volume, including the volume occupied by material of the other field; $\rho' = \rho_1' + \rho_2'$,

p = pressure, assumed to be locally in equilibrium between the two fields, and directly related to the equation of state of the vapor when the droplet field is disperse, or to the maintenance of incompressibility when the droplet field is close packed,

I, T = specific internal energy and temperature, neither of which is likely to be in local equilibrium between the two fields; I and T are related through a specific heat function,

θ = the volume per unit total volume available to the vapor; i.e., porosity or void fraction,

c = local sound speed,

S_{me}, S_{mc} = mass per unit time per unit volume evaporating or condensing, and therefore interchanging between fields,

S_{ie}, S_{ic} = sources to internal energy from evaporation and condensation, including latent heat release or absorption, so that both might have positive and negative contributions,

K = drag function, related to the exchange of momentum between fields,

R = exchange function describing the transfer of heat between fields,

E = heat source, from chemical or nuclear processes,

$\mathbf{V}$ = momentum density source from viscous effects,

V_i = source to internal energy density from viscous dissipation,

r_p = radius of particle, droplet or bubble,

S_p = rate of growth of particle, droplet or bubble scale,

M = the total Mach number for the vapor motion,

D = discrepancy in mass conservation,

$\beta = (\partial D/\partial p)^{-1}$.

In addition to the field variables, we utilize the following nomenclature:

$\mathbf{g}$ = acceleration of gravity,

k = heat conduction coefficient,

ν = kinematic viscosity coefficient,

C_D = drag coefficient,

δt = time increment per calculation cycle,

δr, δz = cross-section dimensions of finite-difference cells,

ω = relaxation parameter for iterative solution,

α_0, β_0 = constants denoting proportions of donor-cell convective fluxing.

Thus, we can write for the density transport equations,

$$\rho_v' = \theta \rho_v , \tag{1}$$

$$\rho_d' = (1 - \theta)\, \rho_d , \tag{2}$$

$$(\partial \rho_{v1}'/\partial t) + \nabla \cdot (\rho_{v1}' \mathbf{u}_v) = S_{me1} - S_{mc1} , \tag{3}$$

$$(\partial \rho_{d1}'/\partial t) + \nabla \cdot (\rho_{d1}' \mathbf{u}_d) = S_{mc1} - S_{me1} , \tag{4}$$

$$(\partial \rho_{v2}'/\partial t) + \nabla \cdot (\rho_{v2}' \mathbf{u}_v) = S_{me2} - S_{mc2} , \tag{5}$$

$$(\partial \rho_{d2}'/\partial t) + \nabla \cdot (\rho_{d2}' \mathbf{u}_d) = S_{mc2} - S_{me2} . \tag{6}$$

Interdiffusion of the component materials in each field has been neglected, but could be included by adding the divergence of a diffusional flux. For the vapor, the distinction between the two components enters the analysis principally as a means for properly calculating the pressure, which requires an equation of state for a mixture of varying proportions. For the droplet field, microscopic incompressibility allows us to write

$$\theta = 1 - (\rho_{d1}'/\rho_1) - (\rho_{d2}'/\rho_2), \tag{7}$$

in which ρ_1 and ρ_2 are the normal material densities of the two components. In some circumstances, it will be important to allow ρ_1 and ρ_2 to vary with temperature, which will permit natural convection in regions where the droplets have coalesced into a continuous fluid.

Next, the momentum equations can be written:

$$\partial(\rho_v'\mathbf{u}_v)/\partial t + \nabla \cdot (\rho_v'\mathbf{u}_v\mathbf{u}_v) = \mathbf{u}_d S_{me} - \mathbf{u}_v S_{mc} - \theta\nabla p + \mathbf{V}_v + \rho_v'\mathbf{g} + K(\mathbf{u}_d - \mathbf{u}_v), \tag{8}$$

$$\partial(\rho_d'\mathbf{u}_d)/\partial t + \nabla \cdot (\rho_d'\mathbf{u}_d\mathbf{u}_d) = \mathbf{u}_v S_{mc} - \mathbf{u}_d S_{me} - (1 - \theta)\nabla p + \mathbf{V}_d + \rho_d'\mathbf{g} + K(\mathbf{u}_v - \mathbf{u}_d). \tag{9}$$

Note that the factors θ and $1 - \theta$ lie outside the pressure gradients. If these were within the gradients as some authors have proposed, then the equations could not represent static equilibrium for an inhomogeneous distribution in the absence of gravity. The way in which the drag function K is introduced is specifically for the purpose of the numerical solution technique, which requires a linearized implicit coupling between fields. It is important to emphasize, however, that this does not require a linear *physical* coupling between fields, only a linear *implicitness*. The K function itself can vary with velocity, and the numerical solution technique can also include the various virtual mass effects and other extensions that are necessary for accurate representation of the dynamics. These matters are discussed further in the next section.

Also, we have the energy equations, which are written in the following form:

$$\rho_v'[(\partial I_v/\partial t) + \nabla \cdot (\mathbf{u}_v I_v) - I_v \nabla \cdot \mathbf{u}_v] = S_{iev} - S_{icv} + E_v + R(T_d - T_v) + K(\mathbf{u}_d - \mathbf{u}_v)^2 + \nabla \cdot (k_v\theta\nabla T_v) + V_{iv} - p\nabla \cdot [\theta\mathbf{u}_v + (1 - \theta)\mathbf{u}_d], \tag{10}$$

$$\rho_d'[(\partial I_d/\partial t) + \nabla \cdot (\mathbf{u}_d I_d) - I_d \nabla \cdot \mathbf{u}_d] = S_{icd} - S_{ied} + E_d + R(T_v - T_d) + \nabla \cdot [k_d(1 - \theta)\nabla T_d] + V_{id}. \tag{11}$$

The heat exchange function R is thus defined as the appropriate variable coefficient by which to multiply the local temperature difference. The effects of drag dissipation have been assigned completely to the heating of the vapor, as also have the work terms arising from both vapor compression and the energy associated with droplet acceleration. The heat-conduction coefficients depend sensitively on θ, with k_d being appreciable only when θ is small (i.e., the droplets are closely packed) and k_v being appreciable only when θ nears unity and the vapor region is fairly continuous and well connected. The source terms from phase transitions are not equal and opposite in their effects, because of the release or absorption of latent heat, burn energy and similar sources.

A variety of equivalent formulations exist for the energy equations, some involving the enthalpy as a field variable, and some being in rigorously conservative form. While these alternatives may have some advantages, our present version is based on ease, numerical stability, accuracy, and efficiency considerations in the numerical solution of the equations.

The Exchange Functions

The two fields are coupled togather through interchanges of mass, momentum and energy, as described by several exchange functions. Such processes as phase transitions or droplet burn affect all three of the conserved quantities, while others such as heat conduction or drag affect only one or two.

Consider first the interchange of mass, as described by the various S functions. For single-component fields, such as pure water droplets in pure steam, the representation of evaporation and condensation is described by rate functions that depend only on temperature and pressure. Momentum and energy interchange carry the specific quantities of the donor field in proportion to the interchange rate for mass, whereas the energy receives an added effect through momentum mixing and the release or absorption of latent heat. For double-component fields, such as a mixture of air and water vapor in one and water droplets with particulate nuclei in the other, the interchange rate also depends crucially on the proportions of the two components for each field, which in turn are modified by unequal depletion or addition rates. A detailed discussion of these complications is beyond the scope of the present paper, in which our principal emphasis is on the description of the solution technique. A goal in the development of this technique, however, has been to include mass interchange among multicomponent fields, so that a later section has been included to show how the basic techniques can be extended to include this capability.

A second interchange is that of momentum, which can occur through two mechanisms. One takes place even in the absence of relative motion between the fields. It results from gradients of pressure, which accelerate the droplets at a different rate from the corresponding acceleration of the vapor. The other momentum exchange can take place even in the absence of pressure gradients, that is, in the absence of macroscopic gradients of the variable we call pressure, which does not include the actual microscopic pressure fluctuations around an individual particle. The first of these mechanisms has sometimes been represented with the porosity function θ *inside* of the gradient operator, but that erroneous form has no basis in physical reality. The second is described in our equations by terms of the form

$$\pm K(\mathbf{u}_v - \mathbf{u}_d).$$

The simplest expression for K, roughly valid for an isolated spherical particle in fairly uniform translation through the vapor, is

$$K = [3\rho_v'(1 - \theta)/2r_p^2\theta](3\nu_v + r_pC_D \mid \mathbf{u}_v - \mathbf{u}_d \mid/4). \tag{12}$$

As discussed by Soo [4] there is also a "force to accelerate the apparent mass of the particle relative to the fluid," and one that "takes into account the effect of the deviation in the flow pattern from steady state." The expressions for these effects involve a time derivative of the relative velocity and an integral of the time derivative. These effects and various other corrections have also been discussed by Corrsin and Lumley [9] for turbulent fluids, but much more research will be required before the effects of turbulence in two-phase momentum transfer can be accurately described in general. A related topic still requiring much investigation occurs when the droplets are deformable, or similarly when bubbles embedded in a liquid are subject to severe deformation during the time-varying dynamics. For this latter case, Eq. (12) must be modified even in the absence of deformation, since it is the droplet field that resists vapor motion, rather than vice versa.

All of these difficulties are severely compounded when the bubbles or droplets are close enough together for interactive effects. In that case, even the simplest expressions without the above-mentioned corrections require modification. A limiting case is that of the flow of liquid through a porous medium, in which case the Darcy drag formula introduces the concept of a permeability that varies strongly with porosity. Soo [4] discusses some representations of the effects in the vicinity of this limit. A very crude approximation to this can be given through the inclusion of an extra factor of θ in the denominator of Eq. (12):

$$K = [3\rho_v'(1 - \theta)/2r_p^2\theta^2](3\nu_v + r_pC_D \mid \mathbf{u}_v - \mathbf{u}_d \mid/4). \tag{13}$$

This form is sufficient to illustrate our numerical solution technique, since any extensions or corrections introduce no further complications. For example, those modifications to $\pm K(\mathbf{u}_v - \mathbf{u}_d)$ that are not proportional to differences in the two velocities can be treated purely explicitly and therefore included in trivial fashion along with the explicitly calculated effects of gravity; whereas, those that are proportional to velocity differences simply modify the variations of K itself, the form of which can be as general as desired in the numerical procedure.

A topic related to the interchange of momentum is that of the particulate, droplet, or bubble scale of size. Equation (13) shows that the drag function depends strongly on this scale, but the dynamics are otherwise not very sensitive to scale variations provided that the size is small compared with the macroscopic geometric features of the system. As long as there is not a localized spread in the distribution of scale, the particulate, droplet, or bubble phase can be treated as a single field. In many circumstances of interest, however, there is a spread to this distribution; that is,

within any small volume there are many different scales for the subdivided phase. An important consequence of this is the resulting spread in velocities, which no longer admits to description by a single field, requiring instead appropriate distribution functions for the field variables, analogous to the Maxwell–Boltzmann distribution for molecular velocities in a gas, but not of so universal a form.

The case of no local spread of scale distribution is easily handled in our present formulation, at least in principle, even if there is considerable variation of scale itself as a function of position and time. All that is required is an appropriate transport equation, which can be written in the form

$$(\partial r_p/\partial t) + \mathbf{u}_d \cdot \nabla r_p = S_p\,, \tag{14}$$

in which S_p describes the rate of scale change resulting from such processes as condensation or evaporation, or possibly from coalescence or fragmentation, although these last tend to spread the distribution of local scale.

One type of coalescence, however, is amenable to treatment by means of a relatively simple extension to our two-field model. In this case, coalescence results in a region of one pure phase with geometrical configuration that is large enough to be resolved numerically in detail. Droplets falling through a vapor, for example, may coalesce into a puddle of progressively increasing depth in the bottom of a vessel, or bubbles rising through water may form into a continuously enlarging vapor pocket above the fluid. The technique for including this sort of process is an important extension to the basic methodology and is described in a later section.

In the energy equations, there is yet another exchange function R defined in such a way that

$$\pm R(T_v - T_d)$$

represents the heat energy transferred per unit volume per unit time between the two fields, as a result of conduction through the exposed surface between them. The details of the process can be quite complicated, especially in the presence of relative motion. For particles in a liquid, the conduction rate depends on the degree of wetting. Three regimes can occur, complete wetting, sporadic wetting, and no wetting. In this last, there is a thin skin of vapor surrounding the particle, which must be very hot in order to sustain the skin, especially when the relative motion is great. Sporadic wetting occurs when the particle is cooler and liquid can occasionally contact its surface, with much resulting agitation of the particle and turbulence in the fluid.

Thus, the formulation of an expression for R is not simple, although various forms have been proposed for special cases. For simple conduction through a layer of effective thickness that is some fraction λ of the particle radius and described

by an effective heat conduction coefficient k_{dv}, R can be estimated by the expression

$$R = 3k_{dv}(1 - \theta)/\lambda r_p^2. \tag{15}$$

More accurate and extensive exchange functions have been discussed by Soo [4], Mecredy and Hamilton [8], Nigmatulin [5], Kalinin [7], and others. From the viewpoint of our numerical solution technique, the incorporation of any appropriate form introduces no significant complications, so that no further discussion of heat exchange is required at this point.

Numerical Procedure

Numerical solutions with a high-speed computer require a means for representing the fields, and a way to calculate changes in the fields through time from a prescribed set of initial conditions, subject to appropriate boundary conditions. To accomplish the representation, we utilize a completely Eulerian mesh of finite-difference cells. In cylindrical coordinates these cells are toroids about the axis, rectangular in cross section and with dimensions δr and δz. Field variables such as p, ρ and I are cell-centered quantities, whereas velocities are located on the sides of cells, as shown in Fig. 1. Integer indices i and j count cell centers in the r and z directions, respectively, whereas half integer indices refer to the cell-edge positions.

To illustrate the methodology, we first omit the exchange of mass between fields, and also assume that there are no macroscopic regions of incompressibility (close-packed droplets). Extensions to include these features will be described in the following section.

Development of the field configurations through time takes place in a sequence of cycles, or time steps, each of duration δt. The steps in each cycle are accomplished

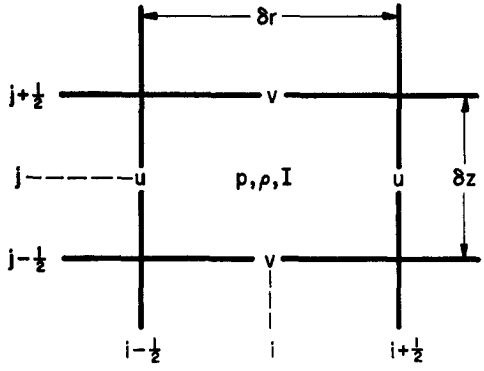

FIG. 1. Layout of field variables and indices for a computational cell.

in such a way as to utilize the results developed in the previous cycle (or the initial conditions) for the calculation of new values of all field variables at a time δt later, and to store these in the computer in such a way that they can be processed yet again in the following cycle.

Calculation of the convective flux of a quantity introduces nomenclature for a partial donor-cell technique, which assists in giving an automatic mitigation of truncation-error effects [10] without the necessity for an explicit artificial diffusion. Angular brackets denote such a donor-cell flux, as exemplified by the following expression for some quantity Q.

$$\langle uQ\rangle^{j}_{i+1/2} \equiv u^{j}_{i+1/2}[(\tfrac{1}{2} + \xi)\, Q_i{}^{j} + (\tfrac{1}{2} - \xi)\, Q^{j}_{i+1}], \tag{16}$$

where ξ is controlled by the specified parameters, α_0 and β_0,

$$\xi \equiv \beta_0 u^{j}_{i+1/2}\, \delta t/\delta r + \alpha_0 \operatorname{sign}(u^{j}_{i+1/2}). \tag{17}$$

The value of α_0 lies between zero (no regular donor cell treatment) and 0.5 (full regular donor cell treatment), and β_0 lies between zero (no interpolated donor cell treatment) and 0.5 (fully interpolated donor cell treatment). For $\alpha_0 = \beta_0 = 0$, the flux is purely space centered, which leads to numerical instability in the absence of a mitigating diffusive process.

The first half of a calculation cycle performs the explicit time advancement of those quantities that do not need to be determined in the implicit iteration loop.

For the components of the droplet field, the transport equations for density can be written in a finite-difference form that ensures the rigorous conservation of mass for each of the two components. Thus, Eqs. (4) and (6) become

$$\begin{aligned} {}^{n+1}(\rho'_{d1})^{j}_{i} = {}^{n}(\rho'_{d1})^{j}_{i} &+ (\delta t/r_i\, \delta r)[\langle u_d r \rho'_{d1}\rangle^{j}_{i-1/2} - \langle u_d r \rho'_{d1}\rangle^{j}_{i+1/2}] \\ &+ (\delta t/\delta z)[\langle v_d \rho'_{d1}\rangle^{j-1/2}_{i} - \langle v_d \rho'_{d1}\rangle^{j+1/2}_{i}], \end{aligned} \tag{18}$$

$$\begin{aligned} {}^{n+1}(\rho'_{d2})^{j}_{i} = {}^{n}(\rho'_{d2})^{j}_{i} &+ (\delta t/r_i\, \delta r)[\langle u_d r \rho'_{d2}\rangle^{j}_{i-1/2} - \langle u_d r \rho'_{d2}\rangle^{j}_{i+1/2}] \\ &+ (\delta t/\delta z)[\langle v_d \rho'_{d2}\rangle^{j-1/2}_{i} - \langle v_d \rho'_{d2}\rangle^{j+1/2}_{i}]. \end{aligned} \tag{19}$$

The superscripts n and $n + 1$ count the cycle numbers; wherever the superscript is omitted the implication is cycle number n.

With these updated densities for the droplet field, Eq. (7) becomes

$${}^{n+1}\theta_i{}^{j} = 1 - {}^{n+1}(\rho'_{d1})^{j}_{i}/\rho_1 - {}^{n+1}(\rho'_{d2})^{j}_{i}/\rho_2\,. \tag{20}$$

In a slightly different form, the equation for one component of the vapor density can be written

$$Q_i^j \equiv [{}^{n+1}(\rho'_{v1})_i^j - {}^{n}(\rho'_{v1})_i^j]/\delta t + (1/r_i\,\delta r)[{}^{n+1}\langle u_v r \rho'_{v1}\rangle_{i+1/2}^j - {}^{n+1}\langle u_v r \rho'_{v1}\rangle_{i-1/2}^j]$$
$$+ (1/\delta z)[{}^{n+1}\langle v_v \rho'_{v1}\rangle_i^{j+1/2} - {}^{n+1}\langle v_v \rho'_{v1}\rangle_i^{j-1/2}] = 0, \tag{21}$$

which differs from Eq. (18) in the advanced-time level of densities and velocities throughout the divergence term. Thus, the equation cannot be solved at this stage of the cycle, but must be deferred until after the determination of advanced-time velocities. An equation for the second component of the vapor field is not used, being replaced by an equation for the sum of the two vapor densities, which is required for implicit coupling with the momentum equation as described below.

A consequence of having transport equations for each material component is the potentiality for fictitious numerical diffusion of one component into another. To preclude this undesirable effect, one could introduce a Lagrangian set of marker particles for each component, which follow the trajectories of individual fluid elements. Indeed, we use such particles anyway for the purpose of visualizing the changing configuration of materials, as illustrated in some of our test-calculation results shown below. Their influence on the calculation would be such as to zero the convective flux of a component into a cell with no marker particles of that component, and to flux all the material of that component from a cell with no marker particles into an appropriate adjacent one with marker particles.

For the internal energy equations we write

$$\begin{aligned}
{}^{n+1}(I_v)_i^j = {}^{n}(I_v)_i^j \Big\{ 1 &+ \frac{\delta t}{r_i\,\delta r}[(ru_v)_{i+1/2}^j - (ru_v)_{i-1/2}^j] + \frac{\delta t}{\delta z}[(v_v)_i^{j+1/2} - (v_v)_i^{j-1/2}] \Big\} \\
&- \frac{\delta t}{r_i\,\delta r}[\langle u_v r I_v\rangle_{i+1/2}^j - \langle u_v r I_v\rangle_{i-1/2}^j] - \frac{\delta t}{\delta z}[\langle v_v I_v\rangle_i^{j+1/2} - \langle v_v I_v\rangle_i^{j-1/2}] \\
&+ \frac{\delta t}{(\rho_v')_i^j} \Big\{ R_i^j[(T_d)_i^j - (T_v)_i^j] + K_i^j[((u_d)_i^j - (u_v)_i^j)^2 + ((v_d)_i^j - (v_v)_i^j)^2] \\
&+ \frac{k_v}{r_i\,\delta r^2}[(\theta r)_{i+1/2}^j((T_v)_{i+1}^j - (T_v)_i^j) - (\theta r)_{i-1/2}^j((T_v)_i^j - (T_v)_{i-1}^j)] \\
&+ \frac{k_v}{\delta z^2}[\theta_i^{j+1/2}((T_v)_i^{j+1} - (T_v)_i^j) - \theta_i^{j-1/2}((T_v)_i^j - (T_v)_i^{j-1})] + (E_v)_i^j \Big\} \\
&- \frac{p_i^j\,\delta t}{(\rho_v')_i^j} \Big\{ \frac{r_{i+1/2}}{r_i\,\delta r}[\theta u_v + (1-\theta)\,u_d]_{i+1/2}^j - \frac{r_{i-1/2}}{r_i\,\delta r}[\theta u_v + (1-\theta)\,u_d]_{i-1/2}^j \\
&+ \frac{1}{\delta z}[\theta v_v + (1-\theta)\,v_d]_i^{j+1/2} - \frac{1}{\delta z}[\theta v_v + (1-\theta)\,v_d]_i^{j-1/2} \Big\},
\end{aligned} \tag{22}$$

$$
\begin{aligned}
{}^{n+1}(I_d)_i^j = {}^n(I_d)_i^j \Big\{ 1 + \frac{\delta t}{r_i\,\delta r}\left[(ru_d)_{i+1/2}^j - (ru_d)_{i-1/2}^j\right] + \frac{\delta t}{\delta z}\left[(v_d)_i^{j+1/2} - (v_d)_i^{j-1/2}\right] \Big\} \\
- \frac{\delta t}{r_i\,\delta r}\left[\langle u_d r I_d\rangle_{i+1/2}^j - \langle u_d r I_d\rangle_{i-1/2}^j\right] - \frac{\delta t}{\delta z}\left[\langle v_d I_d\rangle_i^{j+1/2} - \langle v_d I_d\rangle_i^{j-1/2}\right] \\
+ \frac{\delta t}{(\rho_d')_i^j} \Big\{ R_i^j\left[(T_v)_i^j - (T_d)_i^j\right] + (E_d)_i^j + \frac{k_d}{r_i\,\delta r^2}\left[r_{i+1/2}(1-\theta_{i+1/2}^j)\right. \\
\times \left((T_d)_{i+1}^j - (T_d)_i^j\right) - r_{i-1/2}(1-\theta_{i-1/2}^j)\left((T_d)_i^j - (T_d)_{i-1}^j\right)\Big] \\
\left. + \frac{k_d}{\delta z^2}\left[(1-\theta_i^{j+1/2})\left((T_d)_i^{j+1} - (T_d)_i^j\right) - (1-\theta_i^{j-1/2})\left((T_d)_i^j - (T_d)_i^{j-1}\right)\right] \Big\}. \right. \qquad (23)
\end{aligned}
$$

The time level for K_i^j in this and subsequent parts of the calculation is not of crucial importance; indeed the factors entering into the K_i^j calculation can be mixed in their time levels, with θ_i^j, for example, entering at the $n+1$ level, but the velocity components at the n level.

These finite-difference equations presented so far are in a form that has been demonstrated to work very well in a variety of test problems. Several alternatives exist, especially in the formulation of the convective fluxes. Experience shows that there are several useful guidelines in the choice of these, one being the requirement for the same donor-cell proportions in the fluxes of mass and energy to avoid the tendency to develop inconsistencies in regions where the pressure should remain uniform but mass and energy densities have strong opposing gradients. Another guideline is the utility of convecting specific internal energy, rather than internal energy density, which enables the temperature of an element of material to convect with the material, unless otherwise influenced. Our formulations of the internal energy equations do not ensure the rigorous finite-difference conservation of total energy. The alternative (conservative) technique of deriving changes in internal energy from the difference between changes in total and kinetic energies is highly perilous in both very low-speed flows and highly supersonic flows, being notorious for the inducement of large temperature fluctuations in both extremes.

Despite the importance of correct formulations for these explicit parts of the calculation, they are by no means the crux of our new methodology. The principal numerical problems to be resolved are those of the simultaneous implicit transport of vapor density and the momentum of both fields.

To see how the problem arises and can be efficiently resolved, it is convenient to first introduce special nomenclature for the explicit parts of the momentum equations. For general formulations of the momentum exchange function, the following definitions would include, explicitly, those parts not directly proportional

to the difference in velocity between the two fields. To illustrate the technique with the form in Eq. (13) we define

$$\overline{(\rho_v' u_v)}_{i+1/2}^{j} \equiv (\rho_v' u_v)_{i+1/2}^{j} + (\delta t/r_{i+1/2}\,\delta r)[\langle \rho_v' u_v^2 r\rangle_i^j - \langle \rho_v' u_v^2 r\rangle_{i+1}^j] + (V_{vr})_{i+1/2}^{j}\,\delta t + (\delta t/\delta z)[\langle \rho_v' u_v v_v\rangle_{i+1/2}^{j-1/2} - \langle \rho_v' u_v v_v\rangle_{i+1/2}^{j+1/2}], \tag{24}$$

$$\overline{(\rho_v' v_v)}_{i}^{j+1/2} \equiv (\rho_v' v_v)_{i}^{j+1/2} + (\delta t/r_i\,\delta r)[\langle \rho_v' u_v v_v r\rangle_{i-1/2}^{j+1/2} - \langle \rho_v' u_v v_v r\rangle_{i+1/2}^{j+1/2}] + (V_{vz})_{i}^{j+1/2}\,\delta t + (\delta t/\delta z)[\langle \rho_v' v_v^2\rangle_i^j - \langle \rho_v' v_v^2\rangle_i^{j+1}] + (\rho_v')_i^{j+1/2} g\,\delta t, \tag{25}$$

$$\overline{(\rho_d' u_d)}_{i+1/2}^{j} \equiv (\rho_d' u_d)_{i+1/2}^{j} + (\delta t/r_{i+1/2}\,\delta r)[\langle \rho_d' u_d^2 r\rangle_i^j - \langle \rho_d' u_d^2 r\rangle_{i+1}^j] + (V_{dr})_{i+1/2}^{j}\,\delta t + (\delta t/\delta z)[\langle \rho_d' u_d v_d\rangle_{i+1/2}^{j-1/2} - \langle \rho_d' u_d v_d\rangle_{i+1/2}^{j+1/2}], \tag{26}$$

$$\overline{(\rho_d' v_d)}_{i}^{j+1/2} \equiv (\rho_d' v_d)_{i}^{j+1/2} + (\delta t/r_i\,\delta r)[\langle \rho_d' u_d v_d r\rangle_{i-1/2}^{j+1/2} - \langle \rho_d' u_d v_d r\rangle_{i+1/2}^{j+1/2}] + (V_{dz})_{i}^{j+1/2}\,\delta t + (\delta t/\delta z)[\langle \rho_d' v_d^2\rangle_i^j - \langle \rho_d' v_d^2\rangle_i^{j+1}] + (\rho_d')_i^{j+1/2} g\,\delta t. \tag{27}$$

With these definitions, the equations for total vapor mass and both fields of momentum conservation become

$${}^{n+1}D_i^j \equiv (1/\delta t)[{}^{n+1}(\rho_v')_i^j - {}^{n}(\rho_v')_i^j] + (1/r_i\,\delta r)[{}^{n+1}\langle \rho_v' u_v r\rangle_{i+1/2}^j - {}^{n+1}\langle \rho_v' u_v r\rangle_{i-1/2}^j] + (1/\delta z)[{}^{n+1}\langle \rho_v' v_v\rangle_i^{j+1/2} - {}^{n+1}\langle \rho_v' v_v\rangle_i^{j-1/2}] = 0, \tag{28}$$

$${}^{n+1}(\rho_v' u_v)_{i+1/2}^{j} = \overline{(\rho_v' u_v)}_{i+1/2}^{j} + {}^{n+1}\theta_{i+1/2}^{j}(\delta t/\delta r)({}^{n+1}p_i^{\,j} - {}^{n+1}p_{i+1}^{j}) + K_{i+1/2}^{j}\,\delta t\,[{}^{n+1}(u_d)_{i+1/2}^{j} - {}^{n+1}(u_v)_{i+1/2}^{j}], \tag{29}$$

$${}^{n+1}(\rho_v' v_v)_{i}^{j+1/2} = \overline{(\rho_v' v_v)}_{i}^{j+1/2} + {}^{n+1}\theta_{i}^{j+1/2}(\delta t/\delta z)({}^{n+1}p_i^{\,j} - {}^{n+1}p_i^{j+1}) + K_{i}^{j+1/2}\,\delta t\,[{}^{n+1}(v_d)_{i}^{j+1/2} - {}^{n+1}(v_v)_{i}^{j+1/2}], \tag{30}$$

$${}^{n+1}(\rho_d' u_d)_{i+1/2}^{j} = \overline{(\rho_d' u_d)}_{i+1/2}^{j} + (1 - {}^{n+1}\theta_{i+1/2}^{j})(\delta t/\delta r)({}^{n+1}p_i^{\,j} - {}^{n+1}p_{i+1}^{j}) + K_{i+1/2}^{j}[{}^{n+1}(u_v)_{i+1/2}^{j} - {}^{n+1}(u_d)_{i+1/2}^{j}], \tag{31}$$

$${}^{n+1}(\rho_d' v_d)_{i}^{j+1/2} = \overline{(\rho_d' v_d)}_{i}^{j+1/2} + (1 - {}^{n+1}\theta_{i}^{j+1/2})(\delta t/\delta z)({}^{n+1}p_i^{\,j} - {}^{n+1}p_i^{j+1}) + K_{i}^{j+1/2}[{}^{n+1}(v_v)_{i}^{j+1/2} - {}^{n+1}(v_d)_{i}^{j+1/2}]. \tag{32}$$

The essence of our new methodology lies in the implicitness expressed in these equations, and in the procedure by which these simultaneously coupled equations can be solved for the various $n + 1$ level variables appearing throughout. Throughout the procedure, the proportions of the two vapor components are assumed to remain constant, any requirement for their separate values (e.g., in the equation of state) being satisfied by the n time proportions times the unknown total vapor density. Note that the values of ${}^{n+1}\rho_d'$ have been determined explicitly, so that ${}^{n+1}\theta$ is now also known, and the six unknown quantities to be determined are ${}^{n+1}\rho_v'$, ${}^{n+1}u_v$, ${}^{n+1}v_v$, ${}^{n+1}u_d$, ${}^{n+1}v_d$, and ${}^{n+1}p$. The five equations above, plus the equation of state for the vapor, $p = p(\rho_v, I_v)$, thus make the system exactly determinate, at least in principle. In practice, the solution procedure is moderately complicated, and accordingly is described in some detail. The technique involves an iteration procedure, and we have found the following version to be highly flexible, yet efficient and convenient.

During the iteration, the various field variables accumulate to their final values for the cycle in a series of iterative sweeps during which neither n nor $n + 1$ serves as an appropriate designation. Thus, for these intermediate values we use an over tilde, as for example, $\tilde{p}_i^j$. The first step is an initialization for the six tilde quantities. The simplest one is $(\tilde{\rho}_v')_i^j = {}^n(\rho_v')_i^j$. Experience has shown that pressure initialization should be accomplished in either of two ways, depending on the magnitude of the local Mach number M.

$$\text{As } M_i^j \to 0, \qquad \text{initialize} \quad (\tilde{p})_i^j = {}^n(p)_i^j.$$

$$\text{For } M_i^j \gtrsim 0.1, \qquad \text{initialize} \quad (\tilde{p})_i^j = p[{}^n(\rho_v)_i^j, {}^n(I_v)_i^j].$$

The distinction is essentially that as $M_i^j \to 0$, the manifestations of internal energy fluctuations should not be included in the pressure initialization, the value simply being the result obtained the previous cycle from the iteration convergence, with the equation of state being bypassed at this point. It should be observed, however, that the equation of state is not at all ignored in the vicinity of this limit, but enters crucially into the relationship between changes of density and changes of pressure each step in the iteration. At the limit, $M_i^j = 0$, the effect is to make all changes in microscopic vapor density vanish, as in fact is completely appropriate for incompressible flow, and only at this extreme does the equation of state completely drop out, with the calculation becoming SMAC-like [11]. In general, we initialize the pressure as

$$(\tilde{p})_i^j = f_i^j \, {}^n(p)_i^j + (1 - f_i^j) \, p[{}^n(\rho_v)_i^j, {}^n(I_v)_i^j], \tag{33}$$

where f_i^j is a function of M_i^j that equals unity for $M_i^j = 0$, and decreases mono-

tonically to zero as M_i^j increases. We have found empirically that a useful form is

$$f = [1 + 10(M_i^j/M_0)^4]^{-1}, \tag{34}$$

in which $M_0 = 0.5$. The sound speed c we have used in calculating the local Mach number, is modified from the adiabatic sound speed in the vapor, c_a,

$$c = (c_a/\theta)((\rho_d'/\rho_v') + 1)^{-1/2}, \tag{35}$$

which is the theoretical sound speed in the limit $K \to \infty$. Even if K is not large, this procedure for initialization of the pressure gives good results for all cases we have tested, but one may wish to examine alternative formulations for f in other circumstances.

To complete the initialization, we use the initial densities and pressure in Eqs. (29)–(32), which now become

$$[(\tilde{\rho}_v')_{i+1/2}^j + K_{i+1/2}^j\,\delta t](\tilde{u}_v)_{i+1/2}^j - K_{i+1/2}^j\,\delta t\,(\tilde{u}_d)_{i+1/2}^j$$
$$= (\overline{\rho_v' u_v})_{i+1/2}^j + {}^{n+1}\theta_{i+1/2}^j(\delta t/\delta r)(\tilde{p}_i^{\,j} - \tilde{p}_{i+1}^j), \tag{36}$$

$$[(\tilde{\rho}_v')_i^{j+1/2} + K_i^{j+1/2}\,\delta t](\tilde{v}_v)_i^{j+1/2} - K_i^{j+1/2}\,\delta t\,(\tilde{v}_d)_i^{j+1/2}$$
$$= (\overline{\rho_v' v_v})_i^{j+1/2} + {}^{n+1}\theta_i^{j+1/2}(\delta t/\delta z)(\tilde{p}_i^{\,j} - \tilde{p}_i^{j+1}), \tag{37}$$

$$[{}^{n+1}(\rho_d')_{i+1/2}^j + K_{i+1/2}^j\,\delta t](\tilde{u}_d)_{i+1/2}^j - K_{i+1/2}^j\,\delta t\,(\tilde{u}_v)_{i+1/2}^j$$
$$= (\overline{\rho_d' u_d})_{i+1/2}^j + (1 - {}^{n+1}\theta_{i+1/2}^j)(\delta t/\delta r)(\tilde{p}_i^{\,j} - \tilde{p}_{i+1}^j), \tag{38}$$

$$[{}^{n+1}(\rho_d')_i^{j+1/2} + K_i^{j+1/2}\,\delta t](\tilde{v}_d)_i^{j+1/2} - K_i^{j+1/2}\,\delta t\,(\tilde{v}_v)_i^{j+1/2}$$
$$= (\overline{\rho_d' v_d})_i^{j+1/2} + (1 - {}^{n+1}\theta_i^{j+1/2})(\delta t/\delta z)(\tilde{p}_i^{\,j} - \tilde{p}_i^{j+1}). \tag{39}$$

These must be solved algebraically in pairs for the two components of the velocity in each of the two fields, $\tilde{u}_v$, $\tilde{v}_v$, $\tilde{u}_d$, $\tilde{v}_d$.

Following the initialization, the next step is to derive appropriate equations for the increment to each of the unknown field variables to be added each sweep of the iteration. In previously described techniques such as YAQUI [2], the advancement of the unknown field variables during the iteration is completely incremental. In our present two-field study, this also is possible, but a side effect is the dependence of momentum conservation on the degree of convergence. An alternative procedure, illustrated here, removes this defect. We have tried both in our proof-test studies,

and find negligible difference in the results, so that the choice becomes a matter of convenience and efficiency, which we are not prepared to compare in general for the two techniques.

The nature of this alternative pair of solution techniques becomes apparent when we calculate from Eqs. (29)–(32) the difference in iteration-level values for the variables. Consider, for example,

$$\delta(\tilde{\rho}_v'\tilde{u}_v) \equiv (\tilde{\rho}_v'\tilde{u}_v)^{\text{new}} - (\tilde{\rho}_v'\tilde{u}_v)^{\text{old}},$$

where new and old refer to the newly updated iteration level and the previous iteration level, respectively. Except for the effect of implicit drag coupling, these product functions need not be split, and the direct incremental technique of YAQUI is the natural choice. Here, however, the split cannot be avoided, the increments of ρ and u enter the equations separately. An identity such as

$$\delta(\tilde{\rho}_v'\tilde{u}_v) \equiv \tfrac{1}{2}[(\tilde{\rho}_v')^{\text{new}} + (\tilde{\rho}_v')^{\text{old}}]\,\delta\tilde{u}_v + \tfrac{1}{2}[(\tilde{u}_v)^{\text{new}} + (\tilde{u}_v)^{\text{old}}]\,\delta\tilde{\rho}_v'$$

renders the equations intractable, and must be replaced by the approximation

$$\delta(\tilde{\rho}_v'\tilde{u}_v) \approx (\tilde{\rho}_v')^{\text{old}}\,\delta\tilde{u}_v + (\tilde{u}_v)^{\text{old}}\,\delta\tilde{\rho}_v'$$

in order to proceed with a completely incremental approach. Since the definition and its approximation become the same in the limit of convergence, the two methods produce identical results if the convergence criterion is sufficiently fine. For many purposes, however, tight convergence is not required, so that the slightly longer formulation required for the partially incremental procedure may be counterbalanced by its potentially greater accuracy with fewer iterations.

In both procedures, the first step is to calculate the increment of $\tilde{p}$ for every computational cell. For this we use the Newton–Raphson method for finding the zeros of $\tilde{D}_i^j$, as defined in Eq. (28) in which every $n+1$ value has been replaced by a tilde value. Then,

$$\delta\tilde{p}_i^j = -\omega\beta_i^j\tilde{D}_i^j, \tag{40}$$

in which ω is a parameter whose slight variations above or below unity accomplish over or under relaxation. (Convergence requirements impose limitations on ω that depend on the manner in which the variables are calculated when passing through the mesh of cells.) The field variable β_i^j is defined as

$$\beta_i^j = (\partial\tilde{D}_i^j/\partial\tilde{p}_i^j)^{-1}. \tag{41}$$

Iterative accumulation of changes in the pressure and other field variables continues until $\tilde{D}_i^j$ is sufficiently small, at which time the changes in pressure

according to Eq. (40) are no longer appreciable and the tilde quantities have converged to their final values for the cycle. During the iteration, the internal energy remains constant, so that changes in pressure and vapor density are related by

$$(\rho_v')_i^j = f_i^j \theta_i^j \rho_{v0} + (1 - f_i^j)\tilde{p}_i^j / A_i^j \tag{42}$$

in which ρ_{v0} is a specified density for the incompressible limit ($f_i^j \to 1.0$) and

$$A_i^j \equiv [1/({}^{n+1}\theta_i^j)](\partial \tilde{p}_i^j / \partial \tilde{\rho}_i^j)_{I=\text{const}} \tag{43}$$

can be calculated from the equation of state. This same pressure derivative also occurs in the derivation of an appropriate algebraic form for β_i^j. To accomplish this derivation, it is considerably more convenient to differentiate a slightly different expression for $\tilde{D}_i^j$, namely the form obtained when the mass convection is derived from a strictly centered differencing, with no proportions of donor-cell fluxing. Because the converged solution is independent of β_i^j, it is entirely acceptable to use any desired set of values for this coefficient, provided that the resulting

cycle at those initial values. This same arbitrariness does not, however, apply to the specification of $\tilde{D}_i^j$ as used in Eq. (40); for it the form must be exactly as specified in Eq. (28).

With centered convective flux terms in the $\tilde{D}_i^j$ equation, the necessary derivative is calculated as

$$\begin{aligned}
\frac{1}{\beta_i^j} \equiv \frac{\partial \tilde{D}_i^j}{\partial \tilde{p}_i^j} = {} & \frac{1}{A_i^j\, \delta t} + \frac{\delta t}{r_i\, \delta r}\left\{\frac{1}{\delta r}\left(r_{i+1/2}\,{}^{n+1}\theta_{i+1/2}^j + r_{i-1/2}\,{}^{n+1}\theta_{i-1/2}^j\right)\right. \\
& + r_{i+1/2} K_{i+1/2}^j \frac{\partial}{\partial \tilde{p}_i^j}\left[(\tilde{u}_d)_{i+1/2}^j - (\tilde{u}_v)_{i+1/2}^j\right] \\
& \left. - r_{i-1/2} K_{i-1/2}^j \frac{\partial}{\partial \tilde{p}_i^j}\left[(\tilde{u}_d)_{i-1/2}^j - (\tilde{u}_v)_{i-1/2}^j\right]\right\} \\
& + \frac{\delta t}{\delta z}\left\{\frac{1}{\delta z}\left({}^{n+1}\theta_i^{j+1/2} + {}^{n+1}\theta_i^{j-1/2}\right)\right. \\
& + K_i^{j+1/2} \frac{\partial}{\partial \tilde{p}_i^j}\left[(\tilde{v}_d)_i^{j+1/2} - (\tilde{v}_v)_i^{j+1/2}\right] \\
& \left. - K_i^{j-1/2} \frac{\partial}{\partial \tilde{p}_i^j}\left[(\tilde{v}_d)_i^{j-1/2} - (\tilde{v}_v)_i^{j-1/2}\right]\right\}.
\end{aligned} \tag{44}$$

To complete the derivation requires the velocity derivatives, obtained through

the differentiation of Eqs. (29)–(32), making sure to include the dependence of $(\tilde{\rho}_v')_i^j$ on $\tilde{p}_i{}^j$ through the equation of state. The results of the simultaneous algebraic solution of these equations gives the required pieces for Eq. (44):

$$\frac{\partial}{\partial \tilde{p}_i{}^j}\left[(\tilde{u}_d)_{i+1/2}^j - (\tilde{u}_v)_{i+1/2}^j\right] = \frac{(\tilde{\rho}_v')_{i+1/2}^j\left(1 - {}^{n+1}\theta_{i+1/2}^j\right)\dfrac{\delta t}{\delta r} - {}^{n+1}(\rho_d')_{i+1/2}^j\left(\dfrac{{}^{n+1}\theta_{i+1/2}^j\,\delta t}{\delta r} - \dfrac{(\tilde{u}_v)_{i+1/2}^j}{2A_i{}^j}\right)}{(\tilde{\rho}_v')_{i+1/2}^j\left[{}^{n+1}(\rho_d')_{i+1/2}^j + \delta t\, K_{i+1/2}^j\right] + \delta t\,{}^{n+1}(\rho_d')_{i+1/2}^j\, K_{i+1/2}^j}, \tag{44a}$$

$$\frac{\partial}{\partial \tilde{p}_i{}^j}\left[(\tilde{u}_d)_{i-1/2}^j - (\tilde{u}_v)_{i-1/2}^j\right] = -\frac{(\tilde{\rho}_v')_{i-1/2}^j\left(1 - {}^{n+1}\theta_{i-1/2}^j\right)\dfrac{\delta t}{\delta r} - {}^{n+1}(\rho_d')_{i-1/2}^j\left(\dfrac{{}^{n+1}\theta_{i-1/2}^j\,\delta t}{\delta r} + \dfrac{(\tilde{u}_v)_{i-1/2}^j}{2A_i{}^j}\right)}{(\tilde{\rho}_v')_{i-1/2}^j\left[{}^{n+1}(\rho_d')_{i-1/2}^j + \delta t\, K_{i-1/2}^j\right] + \delta t\,{}^{n+1}(\rho_d')_{i-1/2}^j\, K_{i-1/2}^j}, \tag{44b}$$

$$\frac{\partial}{\partial \tilde{p}_i{}^j}\left[(\tilde{v}_d)_i^{j+1/2} - (\tilde{v}_v)_i^{j+1/2}\right] = \frac{(\tilde{\rho}_v')_i^{j+1/2}\left(1 - {}^{n+1}\theta_i^{j+1/2}\right)\dfrac{\delta t}{\delta z} - {}^{n+1}(\rho_d')_i^{j+1/2}\left(\dfrac{{}^{n+1}\theta_i^{j+1/2}\,\delta t}{\delta z} - \dfrac{(\tilde{v}_v)_i^{j+1/2}}{2A_i{}^j}\right)}{(\tilde{\rho}_v')_i^{j+1/2}\left[{}^{n+1}(\rho_d')_i^{j+1/2} + \delta t\, K_i^{j+1/2}\right] + \delta t\,{}^{n+1}(\rho_d')_i^{j+1/2}\, K_i^{j+1/2}}, \tag{44c}$$

$$\frac{\partial}{\partial \tilde{p}_i{}^j}\left[(\tilde{v}_d)_i^{j-1/2} - (\tilde{v}_v)_i^{j-1/2}\right] = -\frac{(\tilde{\rho}_v')_i^{j-1/2}\left(1 - {}^{n+1}\theta_i^{j-1/2}\right)\dfrac{\delta t}{\delta z} - {}^{n+1}(\rho_d')_i^{j-1/2}\left(\dfrac{{}^{n+1}\theta_i^{j-1/2}\,\delta t}{\delta z} + \dfrac{(\tilde{v}_v)_i^{j-1/2}}{2A_i{}^j}\right)}{(\tilde{\rho}_v')_i^{j-1/2}\left[{}^{n+1}(\rho_d')_i^{j-1/2} + \delta t\, K_i^{j-1/2}\right] + \delta t\,{}^{n+1}(\rho_d')_i^{j-1/2}\, K_i^{j-1/2}}. \tag{44d}$$

Notice that the second and fourth of these are not obtained merely by index changes from the first and third. Equation (44) in all its parts specifies the calculation of $\beta_i{}^j$ for use in Eq. (40), with the result that $\delta\tilde{p}_i{}^j$ is obtainable for every calculation cell and the values of $(\tilde{\rho}_v')_i^j$ can be advanced with Eq. (42). All that remains for the iteration sweep is to advance the four velocity values.

The differentiation that was required for Eqs. (44a)–(44d) is directly applicable for the derivation of the purely incremental procedure for advancing the velocity values. As discussed above, however, we illustrate the alternative derivation for

a partially incremental procedure. For this purpose, Eqs. (29)–(32) are differenced (between two iteration sweeps) in the form

$$(\tilde{\rho}_v{}'\tilde{u}_v)^j_{i+1/2} - K^j_{i+1/2}\,\delta t\,[(\tilde{u}_d)^j_{i+1/2} - (\tilde{u}_v)^j_{i+1/2}] = \bar{R}^j_{i+1/2},$$

$$(\tilde{\rho}_v{}'\tilde{v}_v)^{j+1/2}_i - K^{j+1/2}_i\,\delta t\,[(\tilde{v}_d)^{j+1/2}_i - (\tilde{v}_v)^{j+1/2}_i] = \bar{S}^{j+1/2}_i,$$

$${}^{n+1}(\rho_d{}')^j_{i+1/2}\,(\tilde{u}_d)^j_{i+1/2} - K^j_{i+1/2}\,\delta t\,[(\tilde{u}_v)^j_{i+1/2} - (\tilde{u}_d)^j_{i+1/2}] = \bar{U}^j_{i+1/2},$$

$${}^{n+1}(\rho_d{}')^{j+1/2}_i\,(\tilde{v}_d)^{j+1/2}_i - K^{j+1/2}_i\,\delta t\,[(\tilde{v}_v)^{j+1/2}_i - (\tilde{v}_d)^{j+1/2}_i] = \bar{V}^{j+1/2}_i,$$

in which all the unknown new velocities are isolated on the left side, together with the (already determined) new values of $\tilde{\rho}_v{}'$ and other known quantities. On the right are shorthand expressions involving known tilde quantities from the previous sweep and the known new values for $\delta\tilde{p}_i{}^j$,

$$\bar{R}^j_{i+1/2} = (\tilde{\rho}_v{}'\tilde{u}_v)^j_{i+1/2} + \delta t\,K^j_{i+1/2}(\tilde{u}_v - \tilde{u}_d)^j_{i+1/2} + [\delta t\,(\delta\tilde{p}_i{}^j - \delta\tilde{p}^j_{i+1})/\delta r]\,{}^{n+1}\theta^j_{i+1/2},$$

$$\bar{U}^j_{i+1/2} = {}^{n+1}(\rho_d{}')^j_{i+1/2}\,(\tilde{u}_d)^j_{i+1/2} - \delta t\,K^j_{i+1/2}(\tilde{u}_v - \tilde{u}_d)^j_{i+1/2} + [\delta t\,(\delta\tilde{p}_i{}^j - \delta\tilde{p}^j_{i+1})/\delta r](1 - {}^{n+1}\theta^j_{i+1/2}),$$

$$\bar{S}^{j+1/2}_i = (\tilde{\rho}_v{}'\tilde{v}_v)^{j+1/2}_i + \delta t\,K^{j+1/2}_i(\tilde{v}_v - \tilde{v}_d)^{j+1/2}_i + [\delta t\,(\delta\tilde{p}_i{}^j - \delta\tilde{p}^{j+1}_i)/\delta z]^{n+1}\theta^{j+1/2}_i,$$

$$\bar{V}^{j+1/2}_i = {}^{n+1}(\rho_d{}')^{j+1/2}_i\,(\tilde{v}_d)^{j+1/2}_i - \delta t\,K^{j+1/2}_i(\tilde{v}_v - \tilde{v}_d)^{j+1/2}_i + [\delta t\,(\delta\tilde{p}_i{}^j - \delta\tilde{p}^{j+1}_i/\delta z](1 - {}^{n+1}\theta^{j+1/2}_i).$$

These can be solved as follows:

$$(\tilde{u}_v)^j_{i+1/2} = \frac{{}^{n+1}(\rho_d{}')^j_{i+1/2}\,\bar{R}^j_{i+1/2} + \delta t\,K^j_{i+1/2}(\bar{R}^j_{i+1/2} + \bar{U}^j_{i+1/2})}{(\tilde{\rho}_v{}')^j_{i+1/2}\,[{}^{n+1}(\rho_d{}')^j_{i+1/2} + \delta t\,K^j_{i+1/2}] + \delta t\,{}^{n+1}(\rho_d{}')^j_{i+1/2}\,K^j_{i+1/2}}, \tag{45}$$

$$(\tilde{u}_d)^j_{i+1/2} = \frac{(\tilde{\rho}_v{}')^j_{i+1/2}\,\bar{U}^j_{i+1/2} + \delta t\,K^j_{i+1/2}(\bar{R}^j_{i+1/2} + \bar{U}^j_{i+1/2})}{(\tilde{\rho}_v{}')^j_{i+1/2}\,[{}^{n+1}(\rho_d{}')^j_{i+1/2} + \delta t\,K^j_{i+1/2}] + \delta t\,{}^{n+1}(\rho_d{}')^j_{i+1/2}\,K^j_{i+1/2}}, \tag{46}$$

$$(\tilde{v}_v)^{j+1/2}_i = \frac{{}^{n+1}(\rho_d{}')^{j+1/2}_i\,\bar{S}^{j+1/2}_i + \delta t\,K^{j+1/2}_i(\bar{S}^{j+1/2}_i + \bar{V}^{j+1/2}_i)}{(\tilde{\rho}_v{}')^{j+1/2}_i\,[{}^{n+1}(\rho_d{}')^{j+1/2}_i + \delta t\,K^{j+1/2}_i] + \delta t\,{}^{n+1}(\rho_d{}')^{j+1/2}_i\,K^{j+1/2}_i}, \tag{47}$$

$$(\tilde{v}_d)^{j+1/2}_i = \frac{(\tilde{\rho}_v{}')^{j+1/2}_i\,\bar{V}^{j+1/2}_i + \delta t\,K^{j+1/2}_i(\bar{S}^{j+1/2}_i + \bar{V}^{j+1/2}_i)}{(\tilde{\rho}_v{}')^{j+1/2}_i\,[{}^{n+1}(\rho_d{}')^{j+1/2}_i + \delta t\,K^{j+1/2}_i] + \delta t\,{}^{n+1}(\rho_d{}')^{j+1/2}_i\,K^{j+1/2}_i}, \tag{48}$$

in which the most updated values of $\tilde{\rho}_v{}'$ are to be used.

When this iterative solution has been completed we may now solve for the one remaining unknown field variable ρ'_{v1}, as described by Eq. (21). Again, we employ a simple Newton–Raphson method for finding the zeros of the equation set, $Q_i^j = 0$. The values of $(\tilde{\rho}'_{v1})_i^j$ are initialized at ${}^n(\rho'_{v1})_i^j$, and gradually accumulate to their $n + 1$ time values by increments

$$\delta(\tilde{\rho}'_{v1})_i^j = -\bar{\omega}\bar{\beta}_i^j Q_i^j, \tag{49}$$

in which $\bar{\omega}$, like ω, is an over–under relaxation parameter with value near unity, and

$$(1/\bar{\beta}_i^j) \equiv (1/\delta t) + (1/2r_i\,\delta r)[{}^{n+1}(ru_v)_{i+1/2}^j - {}^{n+1}(ru_v)_{i-1/2}^j] + (1/2\delta z)[{}^{n+1}(v_v)_i^{j+1/2} - {}^{n+1}(v_v)_i^{j-1/2}]. \tag{50}$$

As for β_i^j in the previous iteration, the form for $\bar{\beta}_i^j$ has been obtained by replacing the donor-cell difference form for Q_i^j by a central difference form, but this replacement must not be made in Eq. (49), which requires the full form of Q_i^j obtained from Eq. (21) through replacing $n + 1$ time densities by tilde-level densities. As in the previous iteration, convergence is reckoned by sufficient smallness of the iterative changes, according to whatever criterion of accuracy may be desired.

This completes the derivations necessary to specify a computational cycle. Arrangement of these into a computer code involves numerous additional details [12] not presented here.

Extensions to the Basic Methodology

Two extensions are described in this section, one to allow for the piling up of incompressible fluid into a region fed by the impinging droplets creating a variable boundary position and the other to permit the exchange of mass between fields as, for example, from phase transitions.

The criterion for incompressible pileup is based on the local magnitude of θ. When θ decreases below a preassigned critical value in any computational cell, it is assumed that the droplets have reached a close-packed state, and any further compression is not allowed. For droplets representing an incompressible liquid, the critical value of θ is very small; 0.01 has proved convenient in test problems, with the dynamics of the small vapor residuum being frozen into that of the fluid. For chunks or particles, the critical value of θ may be somewhat larger, leaving appreciable vapor that retains some degree of mobility through the close-packed solid pieces. In this latter case two variants can be distinguished. In one, the solid particles coalesce to form a rigid structure, represented by setting the droplet velocity field to zero and calculating the interpenetrating vapor motion with almost

no change in form to our methodology. In the other, the close-packed solid particles retain a degree of looseness and move about as an incompressible field to which the vapor motion is not completely tied. This somewhat more complicated case requires a separate pressure variable for each field, one to maintain incompressibility in the droplet field of motion, the other to balance Darcy drag, inertial forces, etc., in the vapor field, which in either variant could just as easily be turned into a liquid with its own incompressibility.

Of particular interest for our present purposes has been the case of close pileup of an incompressible liquid with variable boundary position, distinguished on the basis of a very small residual value of θ_i^j. In this case the changes to accomodate such a possibility are easily incorporated as follows.

For every computational cell with θ_i^j exceeding the critical value, the technique remains unchanged. For those in which θ_i^j is less than the critical value, there are several modifications to be made.

(1). The definition of D_i^j for all purposes is changed to

$$D_i^j = (1/r_i\,\delta r)[(u_d r)^j_{i+1/2} - (u_d r)^j_{i-1/2}] + (1/\delta z)[(v_d)_i^{j+1/2} - (v_d)_i^{j-1/2}]. \quad (51)$$

Thus, iteration to the point of vanishing D_i^j for such cells ensures that $\nabla \cdot \mathbf{u}_d = 0$ and the droplet field (not just the individual droplets) is completely incompressible.

(2). The values of A_i^j and K_i^j are set to very large numbers, to tie any residual trapped vapor to the droplet field.

(3). The expression for β_i^j, the pressure iteration coefficient, is vastly simplified to the form

$$\beta_i^j = (\rho_d')_i^j\,\delta r^2\,\delta z^2/[2\delta t(\delta r^2 + \delta z^2)]. \quad (52)$$

The result of these changes is to automatically ensure that the two velocity fields become exactly equal, to order $(K_i^j)^{-1}$. As a result, the drag dissipation in the internal energy equation for the vapor becomes negligible, and indeed the residual trapped vapor becomes completely passive. If the region should again fragment, as signaled by θ_i^j exceeding the critical value, then the standard technique of the previous section is placed in effect again and the fields are free to resume penetration.

The second extension discussed in this section is for the inclusion of mass exchange between fields. The most common example is that of a phase transition, in which, for example, evaporating liquid furnishes a source to the vapor field, building both number and size of the bubbles transported by and through the fluid. Another example is that of particulate burn, as in the propagation of a flame front through gunpowder. In the simplest versions of the former case, the rate of exchange

is such as to maintain local equilibrium between the vapor pressure (a function of temperature) and the local pressure in the fluid and vapor. In the burn example, the exchange must be initiated, and can thereafter be self-sustaining at a rate that depends on temperature. Both cases can be complicated by such matters as the effects of nucleation, depletion and nonequilibrium. A general description of all possibilities is beyond the scope of this present discussion. From the standpoint of precise formulation of the physical process, the task may be quite difficult. In many cases, however, the numerical solution can be accomplished by a relatively simple extension of the basic technique described in the previous section.

Once the various S functions have been derived for the exchange process of interest, their incorporation into the equations can usually be accomplished by means of an explicit subroutine, essentially independent of the other parts of a calculation cycle. In some cases, however, the calculation is much improved by including the vapor density source in the definitions of D, Eq. (28), and Q, Eq. (21), so that these sources enter the implicit iteration procedure.

(1). In each computational cell, mass is added to one field and subtracted from the other, and the densities are accordingly adjusted. Over-depletion can be precluded by implicitness for processes in which the rate depends on the residual amount of a quantity.

(2). The field of r_p values is adjusted to account for growth or decay of the size scale of the particles, droplets or bubbles.

(3). In the cell-size volume surrounding each velocity point, mass exchange carries the velocity of the donor field, leading to a momentum exchange that leaves the donor-field velocity unchanged, but, through momentum mixing with the acceptor field, results in a change in velocity of the latter.

(4). Mass exchange likewise carries the donor-field heat energy to the acceptor field. In addition, there are two other heat sources, one from momentum mixing, which converts kinetic energy to heat, and the other from the release or absorption of the latent heat of a phase transition or from an exothermic or endothermic reaction.

These comments cover, in principle, the modifications necessary to incorporate a mass exchange subroutine. In practice, the calculation can be complicated in at least two respects. For one thing, the rate functions may depend with great sensitivity on the temperature, in which case the presence of small numerical fluctuations in that variable may have very large effects, magnifying to nonsense the small numerical inaccuracies that otherwise would be negligible. A second potential source of difficulty occurs when the exchange rate is extremely rapid, in which case the time step per cycle may have to be cut severely in order to resolve the process. These, however, are difficulties for which additional development in

numerical technology may be required in order to handle some of the more delicate circumstances that can arise.

Examples of Test Calculations

The calculation technique described in this paper has been tested in a variety of circumstances, several of which are described and illustrated here. The calculations were performed with the KACHINA code on a CDC-7600 computer.

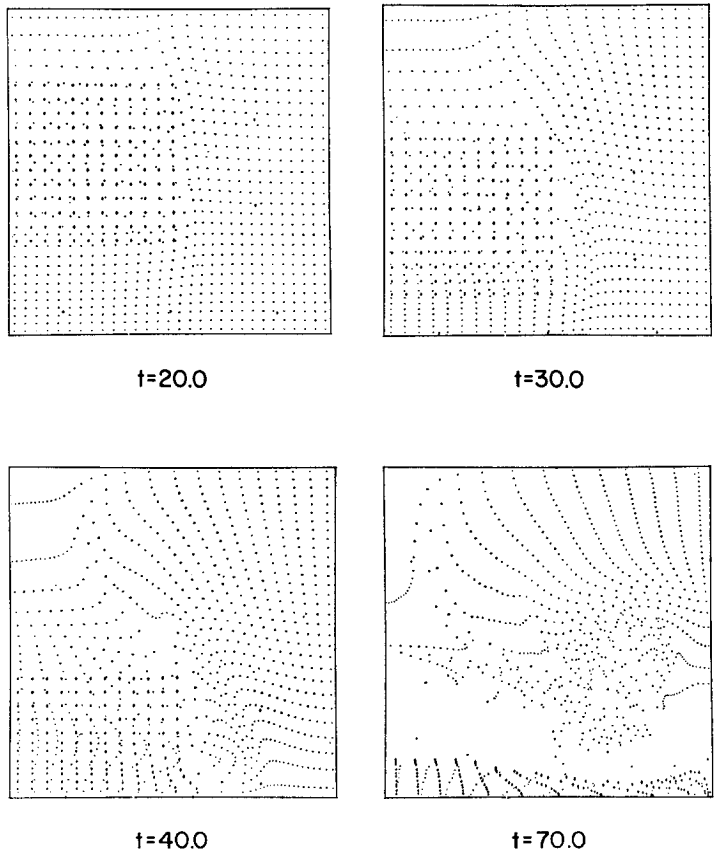

Fig. 2a–e. Calculated results for a cloud of particles falling through vapor, plotted at four different stages in the process: (a) the configuration of marker particles, the dark ones droplets and the light ones vapor; (b) velocity vectors in the vapor field; (c) velocity vectors in the droplet field; (d) contours of vapor density; (e) contours of vapor internal energy.

Typical grind times (computer time in seconds per cycle per finite-difference cell) consistently varied in linear fashion with the number of iterations per cycle, extrapolating to 2.5×10^{-4} sec for no iterations and rising to 6.8×10^{-4} sec for ten iterations. A typical calculation may require only three to four iterations per cycle, sometimes rising appreciably higher, especially if there is some relatively violent transition in the dynamics, as, for example, when a blob of fluid first hits against a rigid wall. Computer-generated plots illustrate the results, summarizing in pictorial form the immense amount of numerical data that can be obtained from each run. These plots include velocity vectors for each field, contour patterns for most of the scalar field variables, and marker-particle configurations following the motion of fluid elements. These last play no computational role in the present

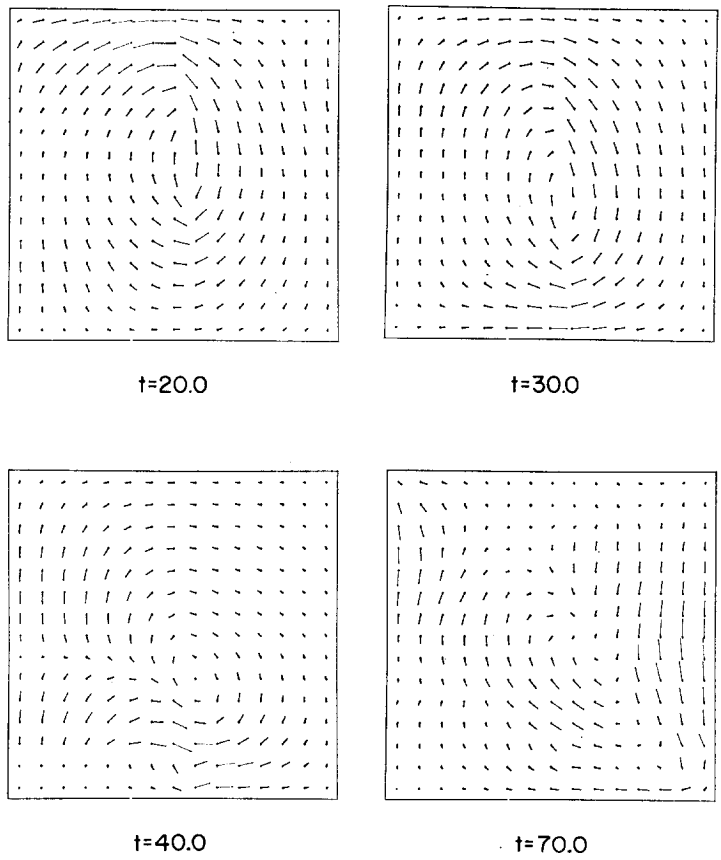

FIGURE 2b. (CONTINUED).

examples, but are of great value for the visualization of results. We have not added any retouching or other alterations to the computer-generated plots reproduced in this paper.

The first calculations we performed were designed to test the accuracy of sound-signal propagation rate. In particular, we examined the motion of a rarefaction front into a region of mixed vapor and droplets, with various magnitudes of the drag function coupling the two fields. Theoretically, we expect the signal speed c to be proportional to the adiabatic sound speed in pure vapor c_a, and also to depend on the void fraction θ, the ratio of material densities, $s = \rho_d/\rho_v$, the drag function K, and the frequency of the sound wave ω. In general, the sound speed is complex, the imaginary part being related to the attenuation rate and to the growth of physical instabilities.

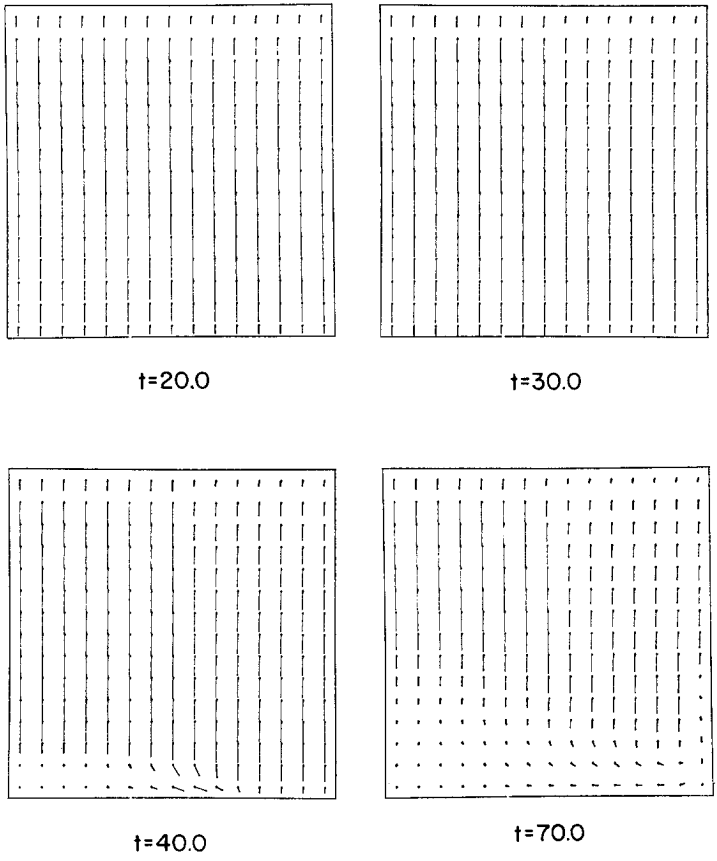

FIGURE 2c. (CONTINUED).

For $K/(\omega\rho_v) \to 0$,

$$c^2 = (c_a^2/s\theta)[\theta(s - 1) + 1], \tag{53}$$

whereas for $K/(\omega\rho_v) \to \infty$,

$$c^2 = (c_a^2/\theta)[s(1 - \theta) + \theta]^{-1}. \tag{54}$$

In both these limits, the sound speed is real, and our tests show that the calculated rate of advancement of a rarefaction front matches the predicted rate for several circumstances investigated.

The second set of tests were designed to match the equilibrium theory for a

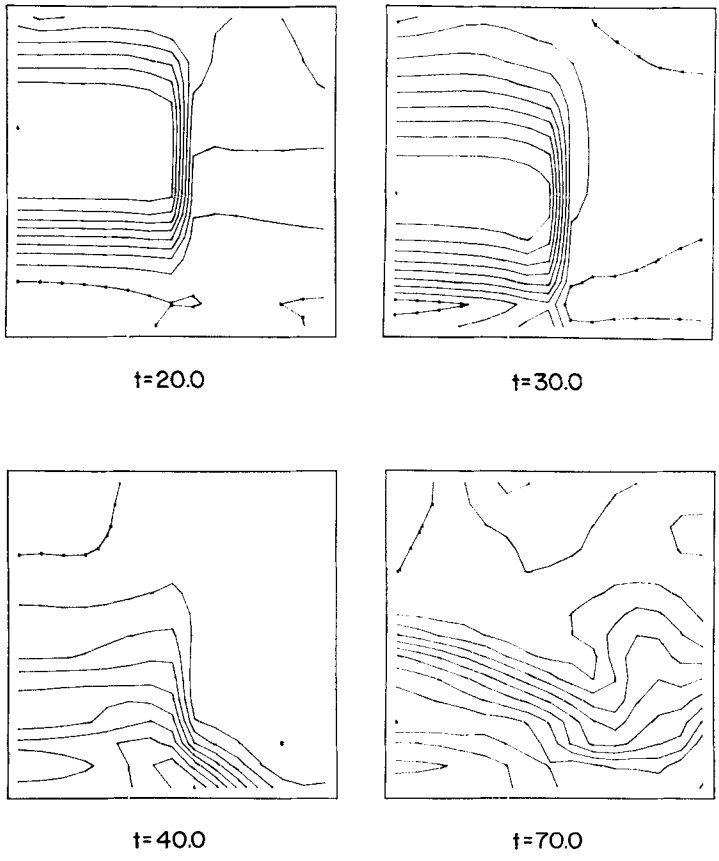

FIGURE 2d. (CONTINUED).

fluidized dust bed, which predicts that when the vapor speed through the bed is u_v, the void fraction is given by

$$\theta(1 - \theta) = u_v K/g(\rho_d - \rho_v), \tag{55}$$

and the pressure gradient by

$$\partial p/\partial x = -g[(1 - \theta)\,\rho_d + \theta\rho_v]. \tag{56}$$

Here g is the (positive) magnitude of the gravitational acceleration, and K can be a function of θ. Perturbation theory, however, indicates the existence of unstable modes, such that the introduction of small oscillations will be followed by an

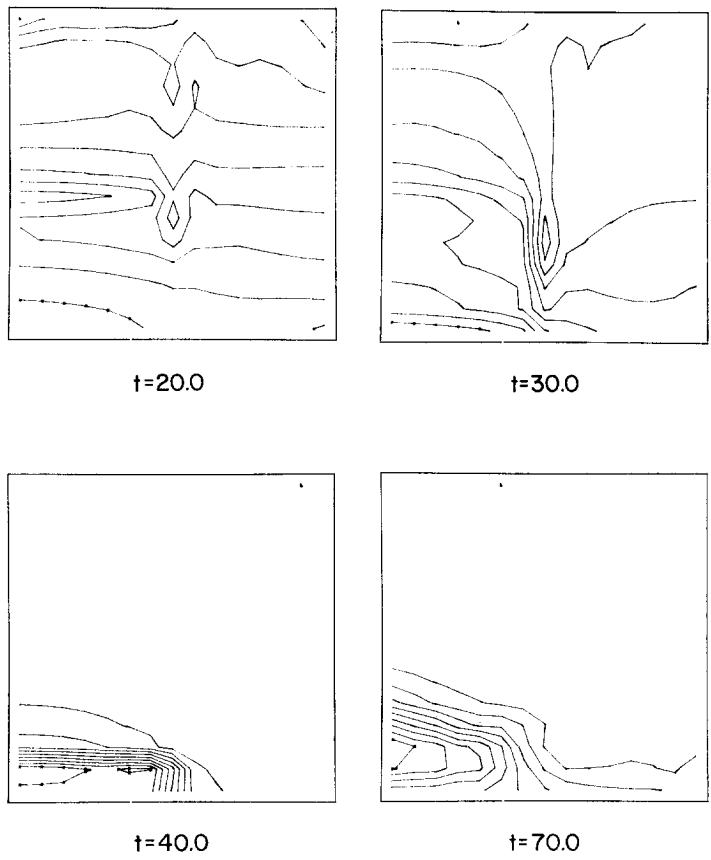

FIGURE 2e. (CONTINUED).

exponential growth of amplitude. Our test involved such a case, with the goal of observing the growth of an instability even in the absence of numerical (computational) instability. We let the calculation introduce the perturbation through the use of varying degrees of coarseness for the iteration convergence criterion. For fine convergence, the numerical calculations held the equilibrium solution for hundreds of calculation cycles. Successively coarser convergence criteria resulted in stronger perturbations from equilibrium and earlier manifestation of the predicted instability. A useful extension of this study would examine the development and migration of bubbles in the bed, as described analytically by Murray [13] and experimentally by Rowe and Partridge [14], from which comparisons could be made among the results of computation, analysis and experiments. At this stage of our testing, however, the only extension we have made to the dust-bed studies was accomplished by suddenly increasing the vapor speed and thereby exhausting the dust from the vessel. Our goal was to prove that the compressed slug of droplets and the following region of essentially pure driving vapor could both be calculated without difficulty. We learned that the expected results could be obtained only by inclusion of the initialization procedure for pressure described by the f function, which was required in order to account for the greatly differing magnitudes of sound speed in the slug and void regions.

The third example discussed here is that of a region of droplets released at the axis of a vessel of vapor. The initial void fraction was great enough to allow the droplets to fall through the vapor, inducing a ring vortex in the latter but scarcely impeding the free fall of the former. In this case, our goal was to test the capability of the calculation for handling the pileup of droplets hitting the bottom of the vessel, with the resulting formation of a splashing puddle of incompressible fluid that forms when the void fraction goes to zero. The results are shown in Fig. 2, in which the cylindrical axis is at the left. Figure 2a illustrates the configurations of the marker particles representing droplets and vapor at a sequence of stages in the falling and splashing. Figures 2b and 2c show corresponding velocity vectors for the two fields. Apparent voids in the vapor at late times are low-density regions heated in the earlier stages by compression and dissipation, and subsequently expanding to give pressure equilibrium. Density and internal energy contour plots for the vapor, Figs. 2d and 2e, show the process more clearly than the marker particles, which are subject to some ambiguity of interpretation when their trajectories have covered large changes in radii.

As a fourth example, we show the effects of sudden induced heating in the central part of a relatively complex initial configuration of materials. The initial conditions are sketched in Fig. 3a. A cylindrical vessel with axis at the left has a rigid bottom and side, and an open top. A liner of incompressible fluid (in this example, devoid of strength effects) surrounds three interior regions. The uppermost of these is essentially pure vapor. Below this are two regions of droplets, both with void

fraction $\theta = 0.4$, and both permeated with vapor. The inner of these is very hot, while the outer is cold, in pressure equilibrium with the liner material and the upper vapor region. The events that develop from this initial state are illustrated in Figs. 3b–3e, which show, respectively, the marker-particle configurations, the vapor field velocity vectors, the droplet field velocity vectors, and the contours of void fraction, each at a sequence of elapsed times. At first, the vapor escapes rapidly from the hot region, developing shocks ahead of its motion and dragging droplets behind. In the upper vapor region, the shock reflects from the massive incompressible liquid liner material. In the lower region, the shock propagates through the cool droplets, piling them against the liner and deforming the latter. Gradually the effects of gravity become apparent, as upthrust droplets fall back and the liner commences to slump. (The visual void above the liner material is not marked by particles, despite the fact that liner material is actually entering the region through the top boundary.) Eventually the whole mass of drops of both kinds has formed into a pair of incompressible fluids, of which the lighter liner material will gradually float on top of the heavier coalesced central droplet material.

Discussion

Both the physical equations and the numerical methodology discussed in this paper are amenable to numerous possible modifications and extensions. This flexibility is ensured by the fact that the interaction functions, material property

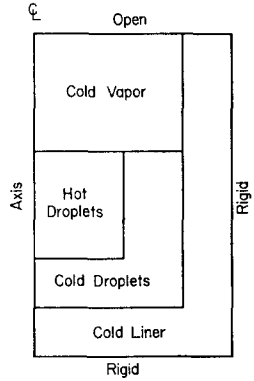

FIG. 3a–e. Calculated results for the explosion and settling of a complex system: (a) a sketch of the initial configuration; (b) sequence of marker particle plots showing vapor (light dots), the central droplets (heavy dots) and the liner droplets (the zeros); (c) the vapor field velocity vectors; (d) the droplet field velocity vectors; (e) the contours of void fraction θ.

descriptions, equation formulations, and similar features do not have to be written in any specific fashion dictated by the technique for solution. This is not to imply that numerical stability and accuracy are ensured for any conceivable innovation that the investigator may wish to insert; careful testing and comparison of results will always be required for this or any other numerical solution procedure. We believe that the principal reason for this degree of flexibility and generality is the strongly implicit coupling among the field variables, which removes many of the restrictions ordinarily encountered in the numerical solution of complicated fluid-flow problems.

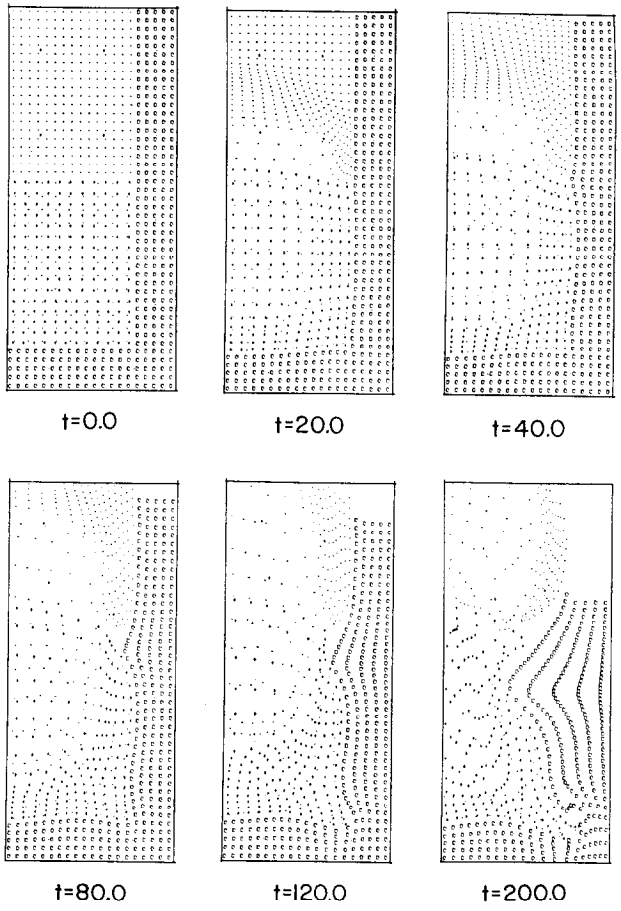

FIGURE 3b. (CONTINUED).

Among the extensions that we plan to develop are many in which the interaction coefficients between fields will be generalized. Another type of extension is to three-field calculations, in which the third field represents a permeable structure with nonisotropic strength, which may soften during heating. For this purpose, strength can be represented by the simple process of holding the third field at rest until it softens, and by incorporating a strength-dependent nonisotropic drag between the third field and each of the others. More generally, the third field may be required to undergo elastic or plastic deformation, but this more complicated capability will require somewhat more development than the rigid-yield model.

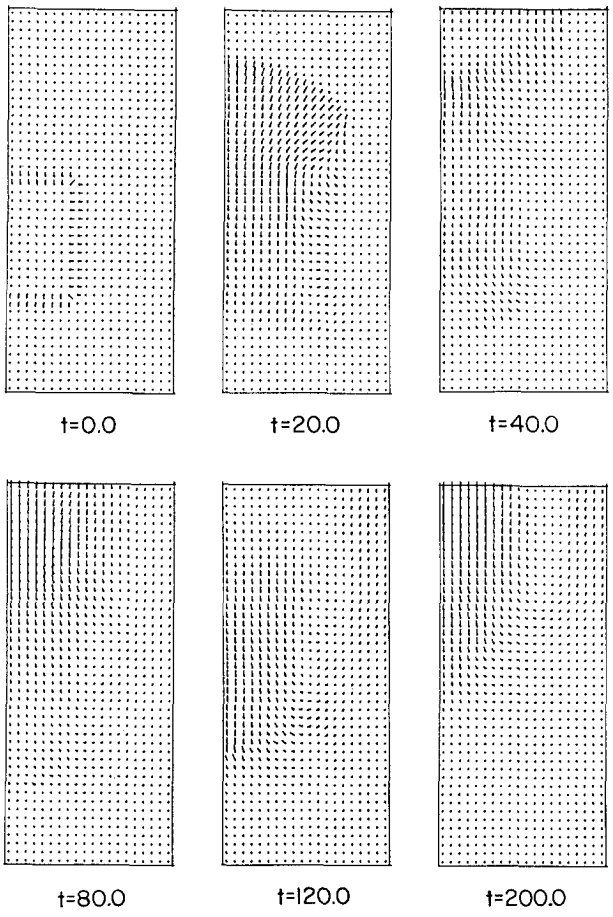

FIGURE 3c. (CONTINUED).

In addition to these and other possible extensions, there is also the possibility for several areas of simplification. One of these is for the case in which both fields are microscopically incompressible. For programs of investigation with this feature, considerable computer-usage efficiency could be realized through the omission or simplification of terms and procedures.

One especially useful conclusion from the development so far has been to clarify the distinction between numerical and physical instability in two-field flows. The differential equations are known to possess complex characteristics, and the linear stability analysis of these equations shows not only circumstances of complex

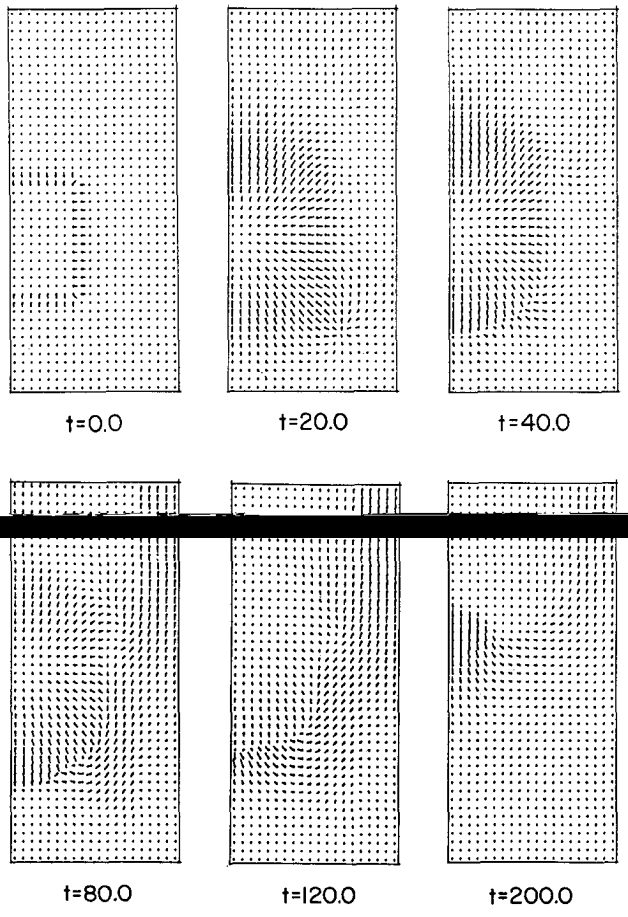

FIGURE 3d. (CONTINUED).

sound speed but also the existence of growing instability in many problems of physical interest [3]. At least two sources exist for these growing modes. One is the effect of the factors θ and $1 - \theta$ modifying the pressure gradients, with results that amplify the tendency for particles to clump together when a homogeneous distribution is perturbed. The other arises from the dependence of K on θ, describing the collective effects of particulate clumping, from which increased drag enhances the process even further.

It is important to recognize that although the highest wave-number perturbations are damped by dissipation (e.g. from viscosity), the remaining instabilities are

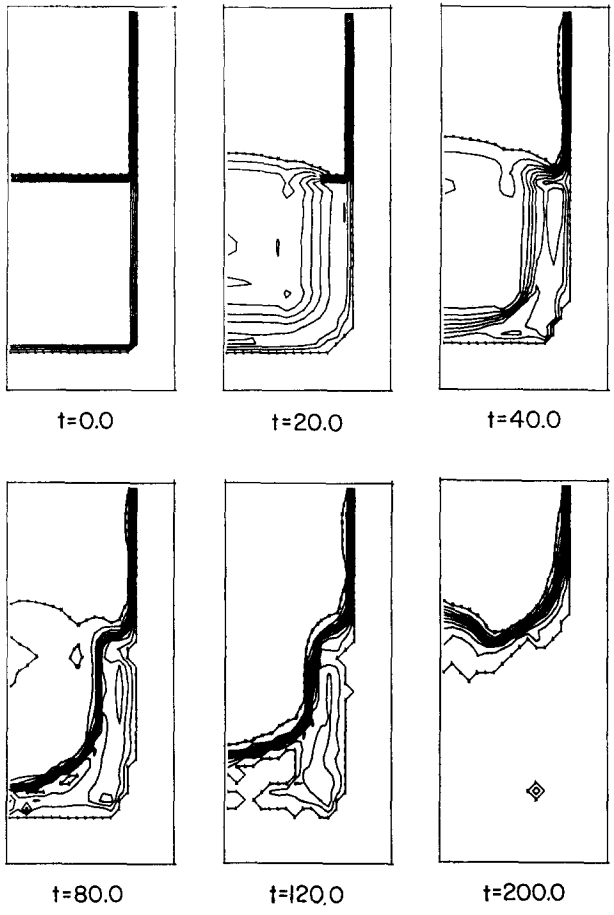

FIGURE 3e. (CONTINUED).

physically real, in contrast to the numerical instabilities that can arise in computer solutions. Although the linearized analysis of infinitesimal perturbations to the differential equations leads to predictions of unmitigated exponential growth, we know from more extended analysis [13] and experiments [14] that the growth of the perturbation is eventually bounded by nonlinear effects.

Numerical solutions must be capable of representing these physical instabilities, and one of our examples has shown that the present technique possesses this capability. In general, the extent to which a given calculation will show such a development depends crucially on the relative time scales for perturbation growth on the one hand and for the completion of the macroscopic flow developments on the other. In our third example, the falling clump of particles hit the bottom of the vessel before the physically disruptive processes could work to distort the orderly droplet array. If the particles were released from much higher, the effects of true physical instability would be felt, and our first example shows that the numerical calculations would, indeed, exhibit this.

REFERENCES

1. F. H. HARLOW AND A. A. AMSDEN, *J. Computational Phys.* **8** (1971), 197.
2. A. A. AMSDEN AND C. W. HIRT, "YAQUI: An Arbitrary Lagrangian–Eulerian Computer Program for Fluid Flow at All Speeds," Los Alamos Scientific Laboratory Report LA-5100, Los Alamos, NM, 1973; C. W. HIRT, A. A. AMSDEN AND J. L. COOK, *J. Computational Phys.* **14** (1974), 227.
3. J. D. MURRAY, *J. Fluid Mech.* **21** (1965), 30.
4. S. L. SOO, "Fluid Dynamics of Multiphase Systems," Blaisdell, Waltham, MA, 1967.
5. R. I. NIGMATULIN, *Fluid Dynamics* **2** (1967), 20. (Translated from *Izv. AN SSSR Mekhanika Zhidkosti i Gaza* **2** (1967), 33.
6. T. B. ANDERSON AND R. JACKSON, *I and EC Fundamentals* **6** (1967), 527.
7. A. V. KALININ, *Heat Transfer-Soviet Research* **2** (1970), 83.
8. R. C. MECREDY AND L. J. HAMILTON, *Internat. J. Heat Mass Transfer* **15** (1972), 61.
9. S. CORRSIN AND J. LUMLEY, *Appl. Sci. Res.*, **6** (1956), 114.
10. C. W. HIRT, *J. Computational Phys.* **2** (1968), 339.
11. A. A. AMSDEN AND F. H. HARLOW, "The SMAC Method: A Numerical Technique for Calculating Incompressible Fluid Flows," Los Alamos Scientific Laboratory Report LA-4370, Los Alamos, NM, 1970.
12. A. A. AMSDEN AND F. H. HARLOW, "KACHINA: An Eulerian Computer Program for Multifield Fluid Flows," Los Alamos Scientific Laboratory Report LA-5680, Los Alamos, N.M., 1974.
13. J. D. MURRAY, *J. Fluid Mech.* **22** (1965), 57.
14. P. N. ROWE AND B. A. PARTRIDGE, *J. Fluid Mech.* **23** (1965), 583; see also *Trans. Inst. Chem. Engrs.* **43** (1965), 157.